# Galvanic Corrosion Behavior of Steam Generator Tube Materials within Pores of Magnetite Deposits in Alkaline Solutions

Soon-Hyeok Jeon*, Geun Dong Song, Do Haeng Hur

*Nuclear Materials Research Division, Korea Atomic Energy Research Institute, 989-111, Daedeok-daero,*
*Yuseong-gu, Daejeon, 34057, Republic of Korea*
*\*Corresponding author: junsoon@kaeri.re.kr*

## 1. Introduction

Magnetite is the main corrosion product released from the surface of carbon steel in a secondary coolant system of the pressurized water reactors (PWRs). The magnetite particles are transported into the steam generators (SGs) and deposited on the surface of SG heat exchanger tubes, top of tube sheet, and tube support structures [1-3]. The magnetite adhering to the SG tubes and tube sheet causes an acceleration of the corrosion rate of the SG structural materials [1-3].

Recently, many researches on the galvanic effect by magnetite on the corrosion behavior of secondary system materials such as nickel based alloys [4-6] and carbon steel [7-9] have been reported. It is well known that the SG deposits are porous in nature and consist of mainly magnetite. Because magnetite has a high electrical conductivity of 0.025 $\mu s$/cm at room temperature [10], an electric contact between SG structural materials and magnetite deposits can be occurred. In various secondary conditions, it was reported that the corrosion potential of magnetite was much higher than those of secondary system materials and the corrosion rate of the materials was increased due to the shift in their potentials to the anodic direction [4-9].

However, except for magnetite, metallic copper and lead were also constituted the SG tube deposits by the reduction of copper and lead oxide, and thus would affect in the corrosion behavior of SG tube materials. Therefore, a need exists to know about the galvanic corrosion behavior between SG materials and corrosion products such as metallic copper and lead particles in the secondary water of PWRs. However, there are few studies for the effect of copper and lead on the galvanic corrosion of SG materials in the simulated secondary water of PWRs.

In this study, the galvanic corrosion behavior of SG tube materials in pores with in the magnetite flakes was investigated in an alkaline solution. The magnetite flake samples taken from an operating SG were analyzed to identify the various corrosion products accumulated in the pores of the flakes. To simulate the magnetite on the surface of SG tube materials, the magnetite films were electrodeposited on the surface of Alloy 690 substrate from a Fe(III)-TEA-based electrolyte. Then, the electrochemical corrosion parameters of SG tube materials and the corrosion products (magnetite, copper, and lead) were measured in the alkaline solution through the various electrochemical techniques.

## 2. Experimental methods

### 2.1. Materials

SG tube materials (Alloy 600 and Alloy 690) and corrosion products (purity 99.99 % copper and lead plates) were cut into a size of 10 x 5 x 1 mm for electrochemical corrosion tests. The specimens were ground using silicon carbide papers down to #1000.

In an operating PWR, SG tube flake samples were collected from the outer surface of SG tubes after Cycle 27 during sludge lancing. The SG model is a Westinghouse model-F and the material of SG heat exchanger tubes is thermally treated Alloy 600. The samples taken from the lancing were dried and stored in an airtight container. The elemental composition of the flakes was analyzed by induced coupled plasma atomic emission spectroscopy (ICP-AES).

### 2.2. Electrodeposition of magnetite film

To evaluate the electrochemical corrosion behavior of magnetite itself, it is necessary to prepare a rigid and dense magnetite electrode. Therefore, a thick magnetite layer was electrochemically deposited on the Alloy 690 substrate. An electrodeposition solution was consisted of 2 M NaOH, 0.1 M triethanolamine (TEA) and 0.043 M $Fe_2(SO_4)_3$. The electrodeposition of magnetite layer was performed using a PAR273 potentiostat with the Power suite software and a three-electrode cell system. A saturated calomel electrode (SCE) was used as a reference electrode and a platinum wire was used as a counter electrode. At an applied potential of $-1.05$ $V_{SCE}$, Magnetite films were electrodeposited on the substrate for 3600 s at 80 $^o$C. After electrodeposition, the magnetite electrodes were rinsed with deionized water and dried in an oven for 5 min at 60 $^o$C.

### 2.3. Microstructural analysis

The SG flakes were ion-milled by a focused ion beam (FIB) to observe the cross-section. The corrosion products and impurities within the pores of flakes were characterized by a scanning electron microscope (SEM) equipped with an energy-dispersive X-ray spectrometer

(EDS). The phase fraction of the flakes was analyzed by a SEM combined with electron back-scatter diffraction (EBSD) analyzer.

## 2.4. Electrochemical tests

The potentiodynamic polarization tests were carried out using a PAR273 potentiostat with Power suite software. An SCE and a platinum wire were used as a reference and counter electrode, respectively. After the open circuit potential (OCP) was stabilized, polarization scans for SG tube materials and corrosion products were started from 10 mV below the OCP to the anodic direction or from 10 mV above the OCP to the cathodic direction. The scan rate was 1 mV/s. Each anodic and cathodic polarization curve was finally combined in one graph. An alkaline aqueous solution of pH 9.0 at 25 ℃ was used in this study. The pH of the test solution was adjusted using ethanolamine (ETA), which is an organic chemical agent used to control the pH of secondary water in PWRs. All electrochemical tests were carried out under a deaerated condition at 80 ℃. Solutions were deaerated by continuously purging with high-purity (99.98 %) nitrogen gas during the tests.

The corrosion current density ($i_{corr}$) of SG materials were determined by means of the Tafel extrapolation of the cathodic and anodic curve between 50 and 100mV away from the corrosion potential ($E_{corr}$). The galvanic potential ($E_{couple}$) and the galvanic current density ($i_{couple}$) of the galvanic couple were calculated from the potentiodynamic polarization curves based on the mixed potential theory.

## 3. Results and Discussion

### 3.1. Characterization of the flakes collected from the SG

The elemental composition of the SG flake samples obtained using ICP-AES is presented in Table I. The values were measured except for oxygen. Based on the ICP-AES data, the main element in the flakes was iron. Trace elements such as manganese, nickel, chromium, copper, titanium, aluminum, and silicon were also observed.

Table I: Elemental analysis of SG magnetite flakes using ICP-AES.

| Element | wt. % |
|---------|-------|
| Fe | 96.68 |
| Mn | 2.02 |
| Ni | 0.62 |
| Cr | 0.07 |
| Cu | 0.32 |
| Ti | 0.18 |
| Al | 0.08 |
| Si | 0.03 |

Fig. 1 shows the cross section of the SG flake observed using SEM. The thickness of the flake was about 120 μm. A large number of the pores were observed on and in the flake sample. The number of pores and pore diameter increased from the tube side to the water side. This result may be closely related to the boiling behavior. The micro-pores of the SG magnetite flakes indicated that the high-temperature water could be exposed to the outer surface of SG tubes through the pores and caused the corrosion reaction.
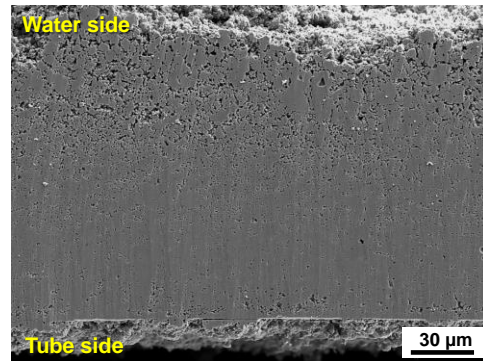


Fig. 1. SEM micrographs of cross section of SG magnetite flake samples.

Fig. 2 shows the EBSD data on the tube side of the SG flakes. As shown in Fig. 2 (a), the analyzed region contained a number of pores. Fig. 2 (b) shows the phase distribution map. Several phases such as magnetite, trevorite, jacobsite, and metallic copper were detected and randomly distributed in all the regions. The flake samples were mainly composed of magnetite (87.59 %) and contained only small amounts of jacobsite (5.61 %), trevorite (4.67 %), and metallic copper particle (2.13 %). In the EBSD results, zero solutions are points in the scan for which no indexing solution could be found for the corresponding pattern [10]. In this flake sample, the micro-pores are represented by the zero solutions. From the EBSD result, it could be confirmed that not only copper particles were precipitated on the surface but also the particles were formed on the inside of the pores.
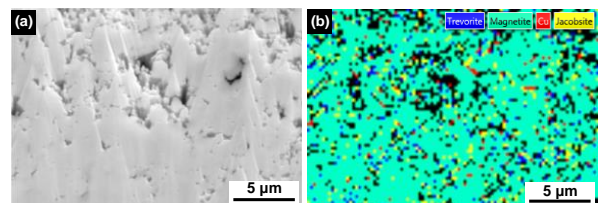


Fig. 2. EBSD data on the tube side of SG magnetite flake samples: (a) SEM micrograph and (b) phase distribution map.

Fig. 3 presents the SEM-EDS analysis of the impurities within the pores on the tube side of the SG flakes. It is well known that the impurities were predominantly concentrated within the pores due to the boiling behavior. The quantitative EDS mapping results are given in Fig. 3. Some impurities such as copper,

lead, chloride, sulfur, and phosphorous were detected within the pores of the SG flake samples. In particular, it can be seen that the concentration of copper and lead was high.
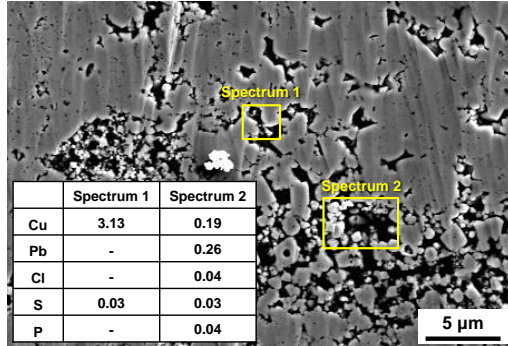


Fig. 3. SEM-EDS analysis of the impurities within the micro-pores formed on the tube side of the SG magnetite flake samples.

From the potential-pH diagrams of the copper-$H_2O$ and lead-$H_2O$ system at 280 ℃, copper and lead are soluble in secondary coolant condition of SG. The pH of the secondary water of SG (pH adjusting agent: ETA, temperature: 280 $^o$C, pH 9.5 at 25 $^o$C) is about 6.14, which was calculated using the MULTEQ code. In the secondary system, the preferred ionic form of copper is $Cu(OH)^+$ and lead is $Pb(OH)^+$. Under the secondary water condition, $Cu(OH)^+$ and $Pb(OH)^+$ can further react to form $Cu(OH)_2$ and $Pb(OH)_2$. These soluble copper and lead species within the pore of magnetite flake could be electrochemically reduced on the outer surface of SG materials through the following reactions.

$$Cu(OH)_2(aq.) + 2H^+ + 2e \rightarrow Cu + 2H_2O \qquad (1)$$
$$Pb(OH)_2(aq.) + 2H^+ + 2e \rightarrow Pb + 2H_2O \qquad (2)$$
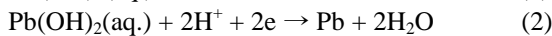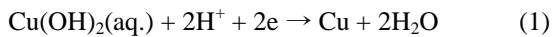
The thermodynamic calculation using the HSC Chemistry 6 software gives $\Delta G_{280℃} = -75.1$ kJ/mol for reaction (1) and $\Delta G_{280℃} = -67.2$ kJ/mol for reaction (2). Based on the results, it is concluded that the reactions for the formation of metallic copper and lead are thermodynamically spontaneous in the secondary system of SG. Therefore, copper and lead are expected to exist in a metallic form in the micro-pores of the magnetite flakes.

*3.2. Electrochemical corrosion behavior of the SG tube materials and corrosion products*

Fig. 4 presents the $E_{corr}$ of the SG tube materials (Alloy 690 and Alloy 600) and the corrosion products (magnetite, copper, and lead) in the alkaline solution at 80 ℃ as a function of time. The $E_{corr}$ of the test materials is ranked in the following order: copper > magnetite > lead > Alloy 600 > Alloy 690. Compare with the $E_{corr}$ of the SG materials, the $E_{corr}$ of the all corrosion products was higher than that of SG materials.
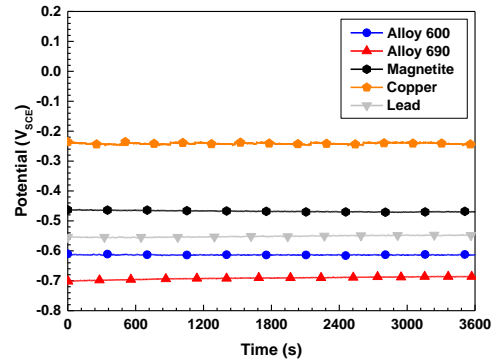


Fig. 4. Corrosion potentials of the SG tube materials and the corrosion products constituting SG magnetite flakes in alkaline solution at 80 $^o$C.

In order to cause the galvanic corrosion between the two or more dissimilar materials, a potential difference (usually > 50 mV [11]) has to exist between the different materials.

Fig. 5 shows the difference of corrosion potentials between the SG tube materials and the corrosion products constituting the magnetite flakes in alkaline solution at 80 ℃. When the corrosion products and SG tube materials are electrically contacted and exposed the same electrolyte, the corrosion products will behave as the cathode of the galvanic couple, while SG tube materials will be the anode and is expected to undergo excessive corrosion.
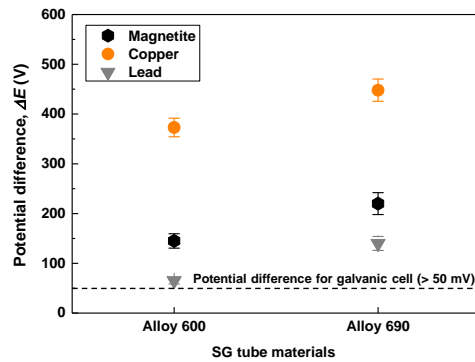


Fig. 5. Corrosion potentials difference between the SG tube materials and the corrosion products constituting the SG magnetite flakes in alkaline solution at 80 $^o$C.

Fig. 6 shows the potentiodynamic polarization curves of the SG tube materials and the corrosion products. The $E_{corr}$ and $i_{corr}$ of SG tube materials were calculated by cathodic Tafel extrapolation. Using the polarization curves of Fig. 6, the galvanic corrosion behaviors between SG tube materials and corrosion products can be measured by using the mixed potential theory. Therefore, in a galvanic couple, the $E_{couple}$ and the $i_{couple}$ are determined by the intersection of the anodic curve of SG tube materials and the cathodic curve of corrosion products, according to the mixed potential theory. When SG tube materials and corrosion products are

galvanically coupled in equal area, the $E_{couple}$ of the SG tube materials is expected to shift in the positive direction and the $i_{couple}$ of SG tube materials is significantly increased by the galvanic coupling. The various electrochemical corrosion parameters obtained from the potentiodynamic curves are summarized in Table II.
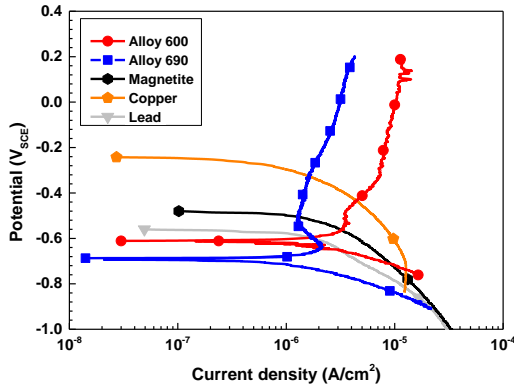


Fig. 6. Potentiodynamic polarization curves of the SG tube materials and the corrosion products in alkaline solution at 80 $^o$C.

Table II. Electrochemical corrosion parameters of SG tube materials in alkaline solution at 80 $^o$C.

| Galvanic coupling | SG tube materials | Corrosion parameters | |
|---|---|---|---|
| | | $E_{corr}$ ($V_{SCE}$) | $i_{corr}$ ($\mu A/cm^2$) |
| Non-coupled | Alloy 600 | −0.61 ±0.01 | 1.62 ± 0.10 |
| | Alloy 690 | −0.69 ±0.01 | 1.05 ± 0.12 |
| Coupled to magnetite | Alloy 600 | −0.56 ± 0.01 | 3.69 ± 0.10 |
| | Alloy 690 | −0.51 ± 0.01 | 1.32 ± 0.13 |
| Coupled to copper | Alloy 600 | −0.39 ± 0.01 | 4.48 ± 0.11 |
| | Alloy 690 | −0.32 ± 0.01 | 1.63 ± 0.12 |
| Coupled to lead | Alloy 600 | −0.59 ± 0.01 | 2.08 ± 0.08 |
| | Alloy 690 | −0.60 ± 0.01 | 2.26 ± 0.12 |

As presented Table II, the corrosion rate of SG tube materials was increased by the galvanic coupling with the magnetite as well as the metallic copper and lead. In the case of area ratio =1, the degree of galvanic effect of Alloy 600 is ranked in the following order: copper > magnetite > lead. And, that of Alloy 690 is in the following order: lead > copper > magnetite. Especially, the galvanic corrosion effect of copper on the all SG tube materials is greater than that of magnetite. For this reason, although the amount of copper and lead contained in the SG deposit is smaller than that of magnetite, galvanic effect of copper and lead should be considered in the corrosion behavior of SG tube.

As a future work, we are planning to study the galvanic effect of corrosion products on other SG structural materials (SG tube sheet and tube support plate) and effect of area ratio between SG materials and corrosion products on galvanic corrosion acceleration.

## 3. Conclusions

The galvanic corrosion of SG tube materials (Alloy 690 and Alloy 600) within the pores of magnetite flakes was investigated in an alkaline solution using the electrochemical tests. The corrosion rate of SG tube materials was increased by the galvanic coupling with the each corrosion products (magnetite, copper, and lead). Based on the results, except for magnetite, galvanic effect of metallic copper and lead particles should be considered in the corrosion behavior of SG tube.

## ACKNOWLEDGEMENTS

## REFERENCES

[1] I. H. Plonski, J. Appl. Electrochem. 27 (1997) 1184-1192.
[2] C. Ramesh, N. Murugesan, A. A. M. Prince, S. Velmurugan, S. V. Narasimhan, V. Ganesan, Corros. Sci. 43 (2001) 1865-1875.
[3] A. A. M. Prince, S. Velmurugan, S. V. Narasimhan, C. Ramesh, N. Murugesan, P. S. Raghavan, R. Gopalan, Nucl. Mater. 289 (2001) 281-290.
[4] S.H. Jeon, G.D. Song, D.H. Hur, Corrosion behavior of Alloy 600 coupled with electrodeposited magnetite in simulated secondary water of PWRs, Mater. Trans. 56 (2015) 2078-2083.
[5] S.H. Jeon, G.D. Song, D.H. Hur, Galvanic corrosion between Alloy 690 and magnetite in alkaline aqueous solutions, Metals 5 (2015) 2372-2382.
[6] G.D. Song, S.H. Jeon, J.G. Kim, D.H. Hur, Synergistic effect of chloride ions and magnetite on the corrosion of Alloy 690 in alkaline solutions, Corrosion 73 (2017) 216-220.
[7] S.H. Jeon, G.D. Song, D.H. Hur, Electrodeposition of magnetite on carbon steel in Fe(III)-triethanolamine solution and its corrosion behavior, Mater. Trans. 56 (2015) 1107-1111.
[8] G.D. Song, S.H. Jeon, J.G. Kim, D.H. Hur, Effect of polyacrylic acid on the corrosion behavior of carbon steel and magnetite in alkaline aqueous solutions, Corrosion 72 (2016) 1010-1120.
[9] G.D. Song, S.H. Jeon, J.G. Kim, Y. H. Son, J. G. Kim. D.H. Hur, Galvanic effect of magnetite on the corrosion behavior of carbon steel in deaerated alkaline solutions under flowing conditions, Corrosion Science 131 (2018) 71-80.
[10] S. I. Wright, M. M. Nowell, S. P. Lindeman, P. P. Camus, M. D. Graef, M. A. Jackson, Ultramicroscopy 159 (2015) 81-94.
[11] K.-H. Tostmann, Korrosion, Wiley-VCH, 2001.